

# The Mirage of Performance Gains: Why Contrastive Decoding Fails to Address Multimodal Hallucination

Hao Yin<sup>1</sup> Gunagzong Si<sup>2</sup> Zilei Wang<sup>3</sup>

## Abstract

Contrastive decoding strategies are widely used to reduce hallucinations in multimodal large language models (MLLMs). These methods work by constructing contrastive samples to induce hallucinations and then suppressing them in the output distribution. However, this paper demonstrates that such approaches fail to effectively mitigate the hallucination problem. The performance improvements observed on POPE Benchmark are largely driven by two misleading factors: (1) crude, unidirectional adjustments to the model’s output distribution and (2) the adaptive plausibility constraint, which reduces the sampling strategy to greedy search. To further illustrate these issues, we introduce a series of spurious improvement methods and evaluate their performance against contrastive decoding techniques. Experimental results reveal that the observed performance gains in contrastive decoding are entirely unrelated to its intended goal of mitigating hallucinations. Our findings challenge common assumptions about the effectiveness of contrastive decoding strategies and pave the way for developing genuinely effective solutions to hallucinations in MLLMs.

## 1. Introduction

The hallucination problem (Li et al., 2023b; Liu et al., 2023a; Lovenia et al., 2023; Gunjal et al., 2023) in multimodal large language models (MLLMs) (Bavishi et al., 2023; Chen et al., 2024a; Ye et al., 2023; Chen et al., 2023a) refers to the generation of outputs that are factually incorrect or misaligned with the input data. This issue arises from challenges in aligning diverse data modalities, such as text and images,

<sup>1</sup>School of Artificial Intelligence and Data Science, University of Science and Technology of China <sup>2</sup>School of Computer Science, University of Science and Technology of China <sup>3</sup>School of Information Science and Technology, University of Science and Technology of China. Correspondence to: Zilei Wang <zl-wang@ustc.edu.cn>.

which amplify reasoning errors. Such hallucinations can have serious consequences in critical domains, including autonomous driving (Mai et al., 2023; Liu et al., 2023c; Chen et al., 2023b; Wu et al., 2023) (e.g., false object detection leading to accidents) and healthcare (Wang et al., 2023; Hu et al., 2023) (e.g., incorrect diagnostic interpretations).

Contrastive decoding methods (Wu et al., 2022; Gupta et al., 2022; Niu et al., 2021) are widely recognized as an effective approach to addressing object hallucination in generative models. As illustrated in Figure 1, these methods construct contrastive samples designed to induce hallucinations, then suppress the corresponding output distributions, ensuring closer alignment between model outputs and visual inputs. Representative approaches within this framework include Visual Contrastive Decoding (VCD) (Leng et al., 2023), Instruction Contrastive Decoding (ICD) (Wang et al., 2024b), and Self-Introspective Decoding (SID) (Huo et al., 2024). Their training-free nature and purported ability to address hallucinations have made them highly regarded in the field.

Although methods like VCD have demonstrated remarkable performance improvements on the POPE benchmark (Li et al., 2023c), we reveal in Section 4 that these results are highly misleading. In reality, these methods fail to effectively address model hallucination. The observed performance gains on the POPE benchmark are primarily driven by two factors:

### Misleading Nature of Performance Improvement

$\mathcal{R}_1$ : A unidirectional adjustment of the model output distribution, which simply biases the model towards producing more "Yes" outputs, leading to a balanced distribution on certain datasets.

$\mathcal{R}_2$ : The adaptive plausibility constraints in these methods degrade the sampling decoding strategy into an approximation of greedy search, resulting in deceptively improved performance.

To expose the misleading nature of the performance improvement in the first scenario, we implemented two forced distribution adjustment algorithms in Section 5.1 to show that the apparent gains of contrastive decoding on the POPE

Benchmark are not genuine. The methods are as follows: (1) Prompt-Based Adjustment, where we added a hint to the instruction, such as *"Whenever possible, please select Yes,"* to bias outputs toward "Yes"; and (2) Output Layer Modification, where we altered the output layer to favor "Yes" when the probabilities for "Yes" and "No" were similar. Although neither method mitigates hallucinations, both achieved performance gains comparable to those of contrastive decoding, confirming that these improvements do not represent a genuine solution to the problem.

To highlight the misleading nature of the performance improvement in the second scenario, we incorporated the adaptive plausibility constraint into the standard sampling strategy and compared its predictions with those from contrastive decoding in Section 5.2. The experimental results reveal that, despite having no theoretical connection to hallucination mitigation, the adaptive plausibility constraint accounts for nearly all the performance gains attributed to contrastive decoding. This finding underscores that the contrastive decoding methods, in essence, fail to mitigate hallucinations.

Overall, this paper makes the following three contributions:

- We identified that the performance improvement of contrastive decoding methods stems from its unidirectional and blunt adjustment of the output distribution, which coincidentally balances the distribution on certain datasets.
- We discovered that another key factor driving the performance gains of contrastive decoding methods is their adaptive plausibility constraints, which streamline the sampling strategy into an approximation of greedy search.
- We developed a series of spurious improvement methods and evaluated their performance against contrastive decoding methods. Our findings convincingly show that contrastive decoding methods do not alleviate hallucinations in any meaningful way.

## 2. Related Work

### 2.1. Multimodal Large Language Models

The evolution of MLLMs (Chen et al., 2024b;c) has progressed from BERT-based decoders (Li et al., 2020; 2021) to advanced LLM architectures (Touvron et al., 2023a;b; Meta, 2024), enabling more effective multimodal relationship modeling (Chiang & Li, 2023; Taori et al., 2023; Bai et al., 2023a). Models such as BLIP-2 (Li et al., 2023a) and MiniGPT-4 (Zhu et al., 2023) employ Q-Former mechanisms to enhance the alignment between visual and textual inputs, facilitating more precise cross-modal interactions. InstructBLIP (Dai & et al., 2023) extends this framework by integrating task-specific instructions, improving the model’s ability to interpret context-sensitive visual semantics. Meanwhile, LLaVA (Liu et al., 2023b; 2024; Li et al., 2024) and Qwen-VL (Bai et al., 2023b) adopt simpler linear projection methods that streamline alignment, leading to superior

performance in vision-language tasks. Despite these advancements, hallucination remains a persistent challenge that warrants further investigation.

### 2.2. Contrastive Decoding Strategies

Contrastive decoding (Yan et al., 2023; Zhibo et al., 2023; Han et al., 2022) are widely recognized as effective in addressing object hallucination in generative models. Visual Contrastive Decoding (VCD) (Leng et al., 2023) addresses object hallucination by comparing output distributions generated from standard visual inputs and distorted visual inputs. This approach reduces the model’s dependence on linguistic priors within integrated LLMs and minimizes the impact of statistical biases in MLLM pretraining corpus. Instruction Contrastive Decoding (ICD) (Wang et al., 2024b), in contrast, focuses on the role of instruction perturbations in amplifying hallucinations. By examining the differences in output distributions between standard and perturbed instructions, ICD detects hallucination-prone content and mitigates its impact effectively.

Building upon these two hallucination mitigation methods, numerous approaches, including Adaptive Focal-Contrast Decoding (HALC) (Chen et al., 2024d), Self-Introspective Decoding (SID) (Huo et al., 2024), and Visual Layer Fusion Contrastive Decoding (VaLiD) (Wang et al., 2024a), have been developed based on similar principles. Although these methods have demonstrated substantial performance improvements on the POPE Benchmark, we will show that these improvements are, in fact, **entirely unrelated to the original objective of hallucination mitigation**.

## 3. Contrastive Decoding for Hallucinations

This section details the components and workflows of three mainstream hallucination mitigation methods: VCD, ICD, and SID. These techniques employ contrastive decoding strategies to reduce hallucinatory content, ensuring outputs align more closely with the visual input.

### 3.1. Vanilla Decoding

We consider a MLLM parametrized by  $\theta$ . The model takes as input a textual query  $x$  and a visual input  $v$ , where  $v$  provides contextual visual information to assist the model in generating a relevant response  $y$  to the textual query. The response  $y$  is sampled auto-regressively from the probability distribution conditioned on the query  $x$  and the visual context  $v$ . Mathematically, this can be formulated as:

$$y_t \sim p_\theta(y_t \mid v, x, y_{<t}) \propto \exp \logit_\theta(y_t \mid v, x, y_{<t}) \quad (1)$$

where  $y_t$  denotes the token at time step  $t$ , and  $y_{<t}$  represents the sequence of generated tokens up to the time step  $(t - 1)$ .

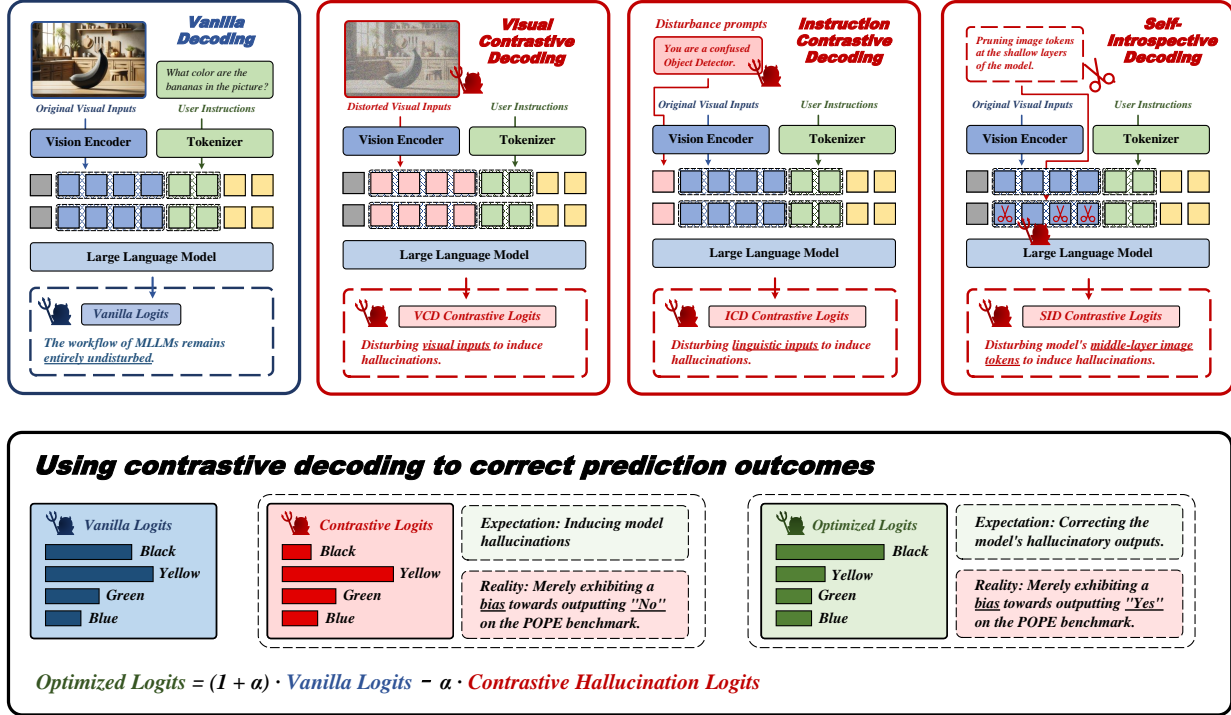


Figure 1. An illustration of hallucination mitigation methods: Visual Contrastive Decoding, Instruction Contrastive Decoding, and Self-Introspective Decoding. The hallucination induction module shifts outputs toward negative responses, while the contrastive decoding module shifts them toward positive responses, rather than achieving their intended effects.

### 3.2. Visual Contrastive Decoding

Visual Contrastive Decoding (VCD) acts as a corrective mechanism, reducing hallucinations by contrasting with distributions derived from distorted visual inputs. Specifically, for a given textual query  $x$  and a visual input  $v$ , the model generates two distinct output distributions: one conditioned on the original  $v$ , and the other on a distorted version  $v'$ . The distorted input  $v'$  is derived by applying predefined perturbations (e.g., a Gaussian noise mask) to  $v$ . Subsequently, a new contrastive probability distribution is computed by leveraging the differences between these two distributions. This contrastive distribution, denoted as  $p_{vcd}$ , is defined as:

$$p_{vcd}(y | v, v', x) = \text{softmax} \left[ \text{logit}_{\theta}(y | v, x) + \alpha \cdot \left( \text{logit}_{\theta}(y | v, x) - \text{logit}_{\theta}(y | v', x) \right) \right], \quad (2)$$

where  $\alpha$  is a hyperparameter controlling the strength of the contrastive adjustment. From the adjusted output distribution  $p_{vcd}$ , **various sampling strategies**, such as nucleus sampling and beam search, can be used to generate text.

A challenge in this process is avoiding indiscriminate penalization of the entire output space, as this could unfairly suppress valid predictions while encouraging the generation of implausible tokens. To address this, VCD integrates an **adaptive plausibility constraint**. This constraint dynam-

ically adjusts penalization based on the confidence levels inferred from the output distribution conditioned on the original visual input  $v$ . The constraint is defined as follows:

$$\mathcal{V}_{\text{head}}(y_{<t}) = \left\{ y_t \in \mathcal{V} \mid p_{\theta}(y_t | v, x, y_{<t}) \geq \beta \max_w p_{\theta}(w | v, x, y_{<t}) \right\}, \quad (3)$$

$$p_{vcd}(y_t | v, v', x) = 0 \text{ if } y_t \notin \mathcal{V}_{\text{head}}(y_{<t}),$$

where  $\mathcal{V}$  denotes the output vocabulary of MLLMs, and  $\beta$  is a hyperparameter that controls the truncation of the next-token distribution. Larger values of  $\beta$  enforce more aggressive truncation, retaining only the tokens with the highest probabilities.

By integrating the contrastive adjustment with the adaptive plausibility constraint, the complete formulation is expressed as follows:

$$y_t \sim \text{softmax} \left[ (1 + \alpha) \cdot \text{logit}_{\theta}(y_t | v, x, y_{<t}) - \alpha \cdot \text{logit}_{\theta}(y_t | v', x, y_{<t}) \right] \quad (4)$$

subject to  $y_t \in \mathcal{V}_{\text{head}}(y_{<t})$ .

### 3.3. Instruction Contrastive Decoding

Based on findings that instruction disturbances with negative prefixes significantly amplify hallucinations by increasing

multimodal alignment uncertainty, Instruction Contrastive Decoding (ICD) mitigates hallucinations by initially emphasizing the probabilities of hallucinated concepts and subsequently detaching these from the original probability distribution. Accordingly, the contrastive distribution,  $p_{icd}$ , can be defined as:

$$p_{icd}(y | v, x, x') = \text{softmax} \left[ \text{logit}_{\theta}(y | v, x) - \lambda \cdot \text{logit}_{\theta}(y | v, x') \right]. \quad (5)$$

A larger  $\lambda$  imposes a stronger penalty on the decisions made by MLLMs under disturbances. Here,  $x'$  represents perturbed instructions involving negative prefixes. Additionally, ICD integrates **adaptive plausibility constraint** from VCD to prevent the unjust suppression of valid predictions.

### 3.4. Self-Introspective Decoding

Building on VCD and ICD, SID recognizes that directly perturbing the entire original input introduces excessive uncertainty and noise, hindering the induction of the desired hallucination effect. To address this, as shown on the far right of Figure 1, SID adjusts the model architecture by retaining only a small subset of image tokens with low attention scores after the early decoder layers. This adaptive mechanism enhances the generation of vision-and-text association hallucinations during auto-regressive decoding. Subsequently, SID isolates these hallucinations from the original probability distribution, leading to the definition of the contrastive distribution  $p_{sid}$  as:

$$p_{sid}(y | v, x) = \text{softmax} \left[ \text{logit}_{\theta}(y | v, x) + \alpha \cdot \left( \text{logit}_{\theta}(y | v, x) - \text{logit}_{\theta'}(y | v, x) \right) \right]. \quad (6)$$

Here,  $\theta'$  represents the MLLM with structural modifications introduced by SID. Additionally, SID incorporates the **adaptive plausibility constraint**

## 4. Misleading Performance Improvement

In this section, we highlight two misleading factors contributing to the performance improvement of contrastive decoding methods on the POPE Benchmark:  $\mathcal{R}_1$ : *Unidirectional output adjustment skews the model towards generating more "Yes" outputs, leading to a balanced distribution in certain datasets.*  $\mathcal{R}_2$ : *The adaptive plausibility constraint degrades sampling decoding strategy into greedy search, resulting in deceptively improved outcomes.*

### 4.1. POPE Benchmark

Polling-based Object Probing Evaluation (POPE) (Li et al., 2023c; Schwenk et al., 2022) is an innovative framework for evaluating object hallucinations in MLLMs. It moves

beyond caption-based methods by treating hallucination detection as a binary task, asking straightforward **Yes-or-No** questions like "Is there a chair in the image?" POPE's performance is assessed through four metrics: Accuracy, Precision, Recall, and F1-score, providing a robust evaluation of hallucination behavior in MLLMs.

Notably, the POPE benchmark ensures a balanced label distribution across all dataset subsets, with "Yes" and "No" samples each constituting 50% of the total.

### 4.2. Unidirectional Output Adjustment

In this subsection, we illustrate how contrastive decoding algorithms can deceptively enhance the performance of MLLMs on the POPE Benchmark by applying targeted, unidirectional modifications to the output distribution. We begin by evaluating the performance of various contrastive decoding methods on the MSCOCO (Lin et al., 2014) and GQA (Hudson & Manning, 2019) datasets, analyzing both accuracy and the distribution of the model's responses.

For this study, we selected LLaVA-v1.5-7B as the foundational MLLM, using a greedy search decoding strategy. The experimental results, summarized in Table 1, show that ICD yielded no performance improvements under this strategy. Consequently, discussions of ICD predictions are temporarily excluded, with the focus shifted to VCD and SID.

Table 1. Performance of various contrastive decoding methods on subsets of POPE Benchmark.

Dataset	MSCOCO-Random		GQA-Adversarial	
Method	Acc (%)	Yes (%)	Acc (%)	Yes (%)
Greedy	87.1 $\uparrow$ 0.0	39.2 $\uparrow$ 0.0	80.9 $\uparrow$ 0.0	54.0 $\uparrow$ 0.0
VCD	88.6 $\uparrow$ 1.5	46.4 $\uparrow$ 7.2	78.0 $\downarrow$ 2.9	63.3 $\uparrow$ 9.3
ICD	86.3 $\downarrow$ 0.8	38.2 $\downarrow$ 1.0	80.9 $\uparrow$ 0.0	52.0 $\downarrow$ 2.0
SID	87.9 $\uparrow$ 0.8	42.3 $\uparrow$ 3.1	79.9 $\downarrow$ 1.0	57.8 $\uparrow$ 3.8

The results reveal that both VCD and SID significantly biased the model's output distribution toward "Yes" across both subsets. On the MSCOCO-Random dataset, where the original output distribution was skewed toward "No," VCD and SID corrected this imbalance, resulting in a more balanced distribution and improved accuracy. Conversely, for the GQA-Adversarial subset, where the output distribution was already biased toward "Yes," these methods intensified the skew, ultimately reducing prediction accuracy.

We further illustrate how model outputs change after applying contrastive decoding methods, providing a clearer understanding of their performance improvements. As shown in Figure 2, the method primarily alters predictions from "No" to "Yes," significantly outpacing the reverse. On the MSCOCO-Random dataset, where the output distribution is initially skewed toward "No," this adjustment converts

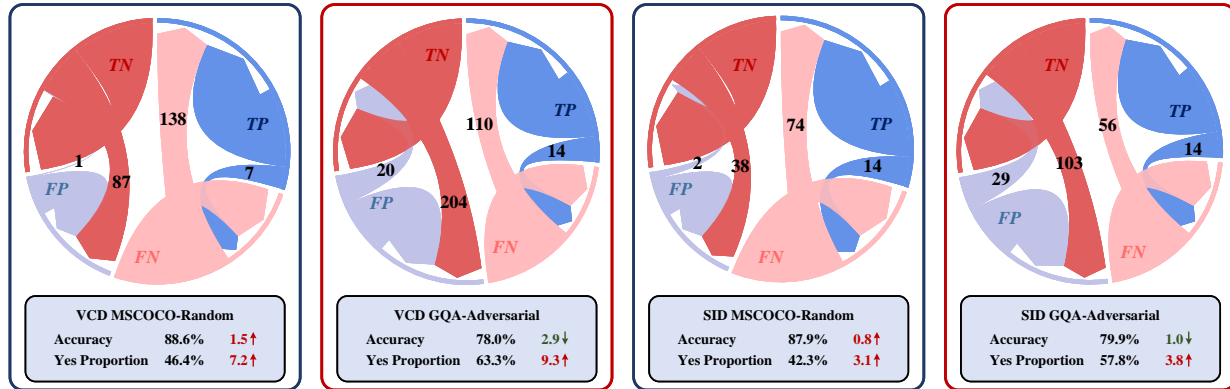


Figure 2. Changes in the distribution of model predictions after applying contrastive decoding methods.

many false negatives into true positives, thereby improving accuracy. Conversely, on the GQA-Adversarial dataset, which is biased toward "Yes," these modifications lead to the misclassification of numerous true negatives as false positives, resulting in a performance decline. For more details on prediction shifts, please refer to Appendix B.

To understand why contrastive decoding methods consistently increase the likelihood of a "Yes" response, we analyzed the output distribution generated from contrastive samples, as shown in Table 2. In Section 3, we proposed that the primary function of contrastive samples is to induce hallucinations, allowing contrastive decoding to subsequently filter out these hallucinated elements from the output distribution. However, the results in Table 2 reveal that this objective was entirely unmet. Most outputs derived from contrastive samples were incorrect—not due to successfully induced hallucinations, but because the model overwhelmingly favored "No" responses. This severe bias in the output distribution led to a significant decline in accuracy.

Table 2. Output distribution generated from contrastive inputs in contrastive decoding methods.

Dataset	MSCOCO-Random		GQA-Adversarial	
Method	Acc (%)	Yes (%)	Acc (%)	Yes (%)
Greedy	87.1 ↑ 0.0	39.2 ↑ 0.0	80.9 ↑ 0.0	54.0 ↑ 0.0
VCD-C	76.7 ↓ 10.4	28.2 ↓ 11.0	71.5 ↓ 9.4	41.3 ↓ 12.7
SID-C	79.0 ↓ 8.1	23.6 ↓ 15.6	74.2 ↓ 6.7	43.1 ↓ 10.9

Based on the above discussion, the practical performance of contrastive decoding methods is illustrated in the lower section of Figure 1. The output distribution derived from the contrastive inputs is heavily biased toward "No." However, the contrastive decoding method suppresses this content in the original output, thereby unilaterally increasing the model’s likelihood of answering "Yes." Whether the model’s performance on the dataset improves depends heavily on whether this increased "Yes" frequency leads to a more

balanced output distribution.

However, as the output distribution of MLLMs tends to be biased toward "No" in most data subsets, contrastive decoding methods still manage to achieve a strong overall performance on the POPE Benchmark. For more details, please refer to Appendix A.

### 4.3. Sampling Decoding Degradation

In this subsection, we will illustrate how contrastive decoding methods misleadingly enhance model performance by degrading sampling-based decoding strategies into greedy search through the adaptive plausibility constraint.

Notably, the POPE Benchmark, which requires models to answer "Yes" or "No," functions as a binary classification task. As a result, greedy search is the most suitable decoding strategy, rendering sampling-based methods unjustifiable. As shown in Table 3, experimental results further confirm that greedy search significantly outperforms sampling. However, many contrastive decoding methods report performance improvements using sampling strategies, necessitating a closer examination of these claims.

Table 3. Performance on the MSCOCO dataset across different decoding strategies.

Model	Decoding	Random	Popular	Adversarial
LLaVA	Greedy	87.1 ↓ 0.0	85.8 ↓ 0.0	83.6 ↓ 0.0
	Sample	83.6 ↓ 3.5	82.4 ↓ 3.4	80.2 ↓ 3.4
QwenVL	Greedy	86.0 ↓ 0.0	85.6 ↓ 0.0	84.0 ↓ 0.0
	Sample	85.2 ↓ 0.8	84.2 ↓ 1.4	82.3 ↓ 1.7

We revisit the **adaptive plausibility constraint** introduced in Section 3.2 and formally defined in Equation (3). This constraint ensures that when the model exhibits high confidence in its outputs corresponding to the original input, the candidate pool is refined to retain only high-probability tokens. By incorporating this mechanism into contrastive

decoding methods, it aims to mitigate adverse effects by preventing the generation of implausible tokens, while safeguarding the coherence and quality of the generated content.

In its original design, the constraint was intended as a complement to contrastive decoding strategies, with **no explicit connection to mitigating hallucinations**. Consequently, it was assumed to have no significant effect when applied independently. However, our findings challenge this assumption: under a sampling strategy, the constraint emerges as a **pivotal** contributor to performance gains.

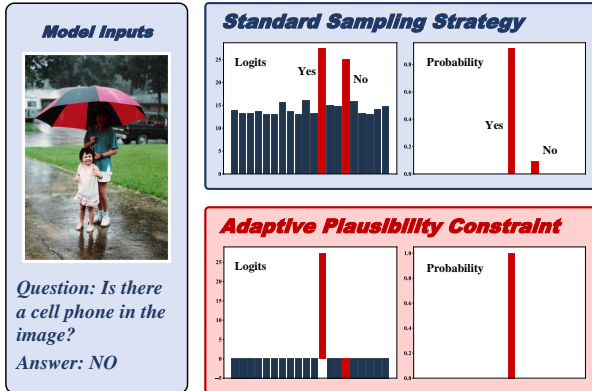


Figure 3. Why does the adaptive plausibility constraint alone result in significant performance improvements?

Figure 3 provides a detailed explanation of why the adaptive plausibility constraint alone significantly improves performance when using the sampling strategy. For the question “Is there a cell phone in the image?”, LLaVA-v1.5-7B model generates the correct output distribution: *Yes*: 8.8% and *No*: 91.2%. Using a greedy search strategy, the model consistently produces the correct answer, “*No*.” However, when employing a sampling strategy, there is an 8.8% chance that the model generates the incorrect answer, “*Yes*.”

When the adaptive plausibility constraint is applied, many candidate options are eliminated by setting their logits to negative infinity for failing to satisfy the condition:

$$p_0(y_t | v, x, y_{<t}) \geq \beta \max_w p_\theta(w | v, x, y_{<t}). \quad (7)$$

Among the excluded candidates is the option “*Yes*.” Consequently, the sampling strategy reduces to a greedy search, ensuring a 100% probability of correctly answering “*No*.”

Consequently, the adaptive plausibility constraint greatly limits the pool of candidate options, transforming the sampling strategy into a predominantly greedy search. As demonstrated in Table 3 and Figure 3, MLLMs exhibit markedly superior performance on the POPE Benchmark under a greedy strategy, underscoring the constraint’s pivotal contribution to performance gains.

This also explains why, in Section 4.2, ICD does not enhance model performance under a greedy search. However, in its original paper, where a sampling strategy was employed, the reported performance gains were much more pronounced.

#### 4.4. Insights

In Section 4.2, we show that when using greedy search as the decoding strategy, contrastive decoding methods modify the model’s predictions in a unidirectional manner, shifting the output distribution toward *Yes*. As a result, performance improvements primarily depend on whether the model’s original output distribution was biased toward *No*.

In Section 4.3, we demonstrate that when sampling is used as the decoding strategy, the adaptive plausibility constraint effectively reduces it to greedy search, serving as a key driver of the observed performance gains.

These findings suggest that the reported improvements from contrastive decoding may be misleading. Specifically, the gains observed on the POPE Benchmark could falsely imply effective hallucination mitigation when, in reality, they stem from unrelated factors.

## 5. Spurious Improvement Methods

In this section, we propose a series of spurious improvement methods based on the two fundamental reasons for performance improvement discussed in Section 4.4. Although these methods are entirely unrelated to hallucination mitigation, they yield experimental results comparable to contrastive decoding techniques. This evidence suggests that while contrastive decoding enhances performance on POPE Benchmark, it does not address hallucinations.

### 5.1. Forced Distribution Adjustment

For the first misleading factor in performance improvement, which involves modifying model predictions in a single direction to bias the output distribution toward “*YES*,” we introduce two pseudo-performance enhancement methods: **Prompt-Based Adjustment** and **Output Layer Modification**, as illustrated in Figure 4.

Prompt-Based Adjustment modifies the input side of the model by appending an additional prompt, “Answer Yes if possible,” after the user’s instruction. This extra input biases the model’s output distribution toward “*Yes*.”

Output Layer Modification refers to adjustments made at the output stage of the model. After generating its initial prediction, the model evaluates the probabilities of “*Yes*” and “*No*.” If their difference is small, i.e.,

$$|p_\theta(\text{Yes} | v, x) - p_\theta(\text{No} | v, x)| < \tau, \quad (8)$$

the prediction is forcibly set to “*Yes*.” Here,  $\tau$  controls how

Table 4. Performance of Prompt-Based Adjustment (PBA) and Output Layer Modification (OLM) on MSCOCO dataset.

Category	Method	LLaVA-v1.5-7B			LLaVA-v1.5-13B			QwenVL-Chat-7B		
		Accuracy	F1-Score	Yes(%)	Accuracy	F1-Score	Yes(%)	Accuracy	F1-Score	Yes(%)
Random	Greedy	87.1	85.5	39.2	86.7	85.0	38.7	85.9	84.0	37.8
	VCD	88.6	88.2	46.4	89.2	88.5	44.4	87.7	86.4	40.6
	SID	87.9	86.9	42.4	87.2	86.2	42.5	86.5	85.3	39.9
	PBA	<b>87.6</b>	<b>86.3</b>	<b>40.2</b>	<b>90.2</b>	<b>89.7</b>	<b>45.7</b>	<b>87.3</b>	<b>86.2</b>	<b>41.5</b>
	OLM	<b>89.6</b>	<b>89.0</b>	<b>44.2</b>	<b>90.0</b>	<b>89.9</b>	<b>48.8</b>	<b>88.2</b>	<b>87.3</b>	<b>43.8</b>
Popular	Greedy	85.8	84.3	40.4	86.0	84.3	39.4	85.6	83.6	38.2
	VCD	86.2	86.0	48.8	87.3	86.8	46.3	87.1	85.9	41.2
	SID	85.1	84.4	45.1	85.1	84.3	44.6	85.3	84.2	39.8
	PBA	<b>86.2</b>	<b>85.0</b>	<b>41.6</b>	<b>88.4</b>	<b>88.1</b>	<b>47.5</b>	<b>86.8</b>	<b>85.5</b>	<b>42.3</b>
	OLM	<b>87.3</b>	<b>86.9</b>	<b>46.5</b>	<b>88.6</b>	<b>88.6</b>	<b>50.2</b>	<b>87.4</b>	<b>86.7</b>	<b>44.8</b>
Adversarial	Greedy	83.6	82.3	42.6	84.3	82.7	41.0	84.0	82.2	39.7
	VCD	<b>81.9</b>	<b>82.5</b>	<b>53.1</b>	<b>83.8</b>	<b>83.8</b>	<b>49.7</b>	84.5	83.4	43.7
	SID	82.3	82.0	47.9	82.9	82.3	46.9	83.2	82.1	42.5
	PBA	<b>83.7</b>	<b>82.7</b>	<b>44.0</b>	<b>84.5</b>	<b>84.7</b>	<b>51.3</b>	<b>84.1</b>	<b>83.2</b>	<b>45.2</b>
	OLM	<b>83.6</b>	<b>83.6</b>	<b>50.1</b>	<b>83.9</b>	<b>84.7</b>	<b>54.9</b>	<b>84.8</b>	<b>84.5</b>	<b>48.4</b>

close the probabilities must be to trigger this modification. This adjustment significantly increases the likelihood of the model predicting "Yes."

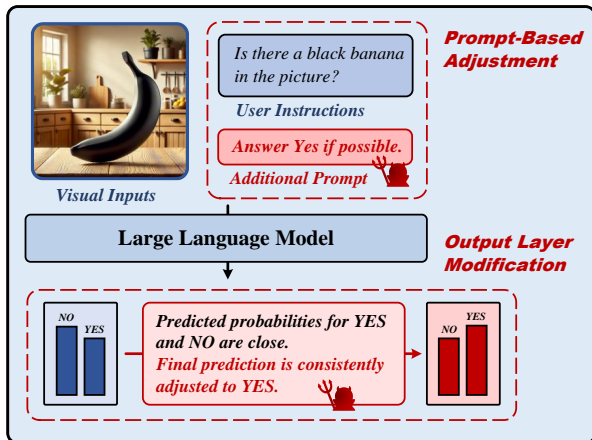


Figure 4. Schematic Diagram of the Prompt-Based Adjustment and Output Layer Modification Algorithm.

**Experimental Settings.** We selected QwenVL-7B, LLaVA-v1.5-7B, and LLaVA-v1.5-13B as the backbone MLLMs. For decoding, we employed a greedy search strategy. Our experiments were conducted on COCO dataset, where the raw output distribution of MLLMs tends to be biased toward "No." As a result, all contrastive decoding methods exhibited notable performance improvements on this dataset.

**Results and analysis.** The experimental results, presented in Table 4, clearly show that PBA achieves an even greater performance improvement than SID, while OLM surpasses VCD. Prediction accuracy increases as the output distribution approaches balance. However, as highlighted in

red, when the distribution shifts beyond balance and biases toward "Yes," accuracy begins to decline again, perfectly aligning with the conclusion in Section 4.4.

Although PBA and OLM are not designed for hallucination mitigation, they produce results similar to contrastive decoding methods, strongly suggesting that contrastive decoding does not effectively address hallucinations. For the experimental results on the AOKVQA and GQA datasets, please refer to Appendix C.

## 5.2. Standalone Application of the Constraint.

The second misleading factor contributing to performance improvement is that the adaptive plausibility constraint degrades the sampling strategy into a greedy search strategy.

To investigate this, we plan to apply the adaptive plausibility constraint in isolation while using sampling as the decoding strategy. This will demonstrate the significant performance gains that occur when the constraint forces the sampling strategy to behave like greedy search. When the adaptive plausibility constraint is applied independently, the model's output distribution can be defined as:

$$\begin{aligned}
 y_t &\sim p_\theta(y_t | v, x, y_{<t}) \\
 &\propto \exp(\text{logit}_\theta(y_t | v, x, y_{<t})), \\
 y_t &\in \mathcal{V}_{\text{head}}(y_{<t})
 \end{aligned} \tag{9}$$

**Experimental Settings.** We utilize LLaVA-v1.5-7B and LLaVA-v1.5-13B as our foundational MLLMs, employing a sampling decoding strategy. Our experiments are conducted on the GQA dataset, where the original output distribution of MLLMs is relatively balanced. Consequently, the modification introduced by contrastive decoding methods,

Table 5. Influence of Independent Application of the Adaptive Plausibility Constraint on Model Performance. **Sample**<sup>†</sup> refers to the sampling strategy that applies the adaptive plausibility constraint independently.

Category	Method	LLaVA-v1.5-7B			LLaVA-v1.5-13B			QwenVL-Chat-7B		
		Accuracy	F1-Score	Yes(%)	Accuracy	F1-Score	Yes(%)	Accuracy	F1-Score	Yes(%)
Random	sample	83.8 ↑ 0.0	83.1	45.6	84.6 ↑ 0.0	83.9	45.9	81.5 ↑ 0.0	79.6	41.1
	VCD	86.6 ↑ 2.8	86.9	52.5	86.7 ↑ 2.1	86.7	49.5	83.8 ↑ 2.3	82.7	44.0
	ICD	85.2 ↑ 1.4	84.5	47.0	85.8 ↑ 1.2	85.0	44.9	82.5 ↑ 1.0	81.8	42.0
	SID	84.9 ↑ 1.1	84.8	49.1	86.0 ↑ 1.4	86.0	49.8	82.9 ↑ 1.4	82.5	43.5
	sample <sup>†</sup>	<b>85.4 ↑ 1.6</b>	<b>84.7</b>	<b>45.1</b>	<b>86.1 ↑ 1.5</b>	<b>85.4</b>	<b>45.3</b>	<b>83.0 ↑ 1.5</b>	<b>82.0</b>	<b>41.8</b>
Popular	sample	77.3 ↑ 0.0	77.8	52.1	80.6 ↑ 0.0	80.6	49.9	76.8 ↑ 0.0	75.9	46.1
	VCD	78.7 ↑ 1.4	80.4	59.4	82.9 ↑ 2.3	83.3	52.4	78.2 ↑ 1.4	78.1	49.4
	ICD	78.1 ↑ 0.8	79.3	54.0	81.5 ↑ 0.9	81.3	49.3	77.5 ↑ 0.7	76.8	47.2
	SID	78.4 ↑ 1.1	79.1	53.7	82.5 ↑ 1.9	83.0	53.3	77.9 ↑ 1.1	77.5	48.0
	sample <sup>†</sup>	<b>78.6 ↑ 1.3</b>	<b>79.6</b>	<b>52.0</b>	<b>81.8 ↑ 1.2</b>	<b>81.8</b>	<b>49.6</b>	<b>78.1 ↑ 1.3</b>	<b>77.0</b>	<b>46.8</b>
Adversarial	sample	75.1 ↑ 0.0	76.1	54.1	78.2 ↑ 0.0	78.9	53.2	76.4 ↑ 0.0	75.3	45.5
	VCD	76.4 ↑ 1.3	79.1	62.5	80.3 ↑ 2.1	81.6	57.0	78.6 ↑ 2.2	78.5	49.2
	ICD	75.8 ↑ 0.7	76.6	54.2	79.2 ↑ 1.0	79.8	52.8	76.8 ↑ 0.4	76.1	46.0
	SID	76.3 ↑ 1.2	77.8	57.5	78.7 ↑ 0.5	80.1	57.5	77.2 ↑ 0.8	76.9	47.5
	sample <sup>†</sup>	<b>76.3 ↑ 1.2</b>	<b>77.3</b>	<b>54.2</b>	<b>79.5 ↑ 1.3</b>	<b>80.1</b>	<b>53.1</b>	<b>77.9 ↑ 1.5</b>	<b>76.5</b>	<b>46.2</b>

which shifts the output distribution towards "Yes," does not introduce a positive bias. However, since the adaptive plausibility constraint converts the sampling strategy into a greedy search, the model's performance still improves.

**Results and analysis.** The experimental results in Table 5 show that when MLLMs adopt sampling as the decoding strategy, applying the adaptive plausibility constraint alone yields an approximate 2.5% performance improvement, effectively validating the conclusion in Section 4.4. Notably, since the adaptive plausibility constraint is entirely unrelated to hallucination mitigation yet achieves performance on par with various contrastive decoding methods, this strongly suggests that contrastive decoding methods do not actually mitigate hallucinations. For the experimental results on the AOKVQA and COCO datasets, please refer to Appendix D.

## 6. Discussion on Hallucination Mitigation

Based on the insights from Sections 4 and 5, we propose some new criteria for evaluating hallucination mitigation.

**Impact of Decoding Strategies.** When evaluating on POPE Benchmark, it is essential to account for the substantial influence of different decoding strategies on model performance. Notably, greedy search consistently outperforms sampling-based approaches such as nucleus sampling and beam search. If a hallucination mitigation method involves modifications to the sampling module, careful consideration must be given to whether these changes affect the core properties of the decoding strategy.

**Avoiding Unidirectional Modification.** When evaluat-

ing hallucination mitigation methods, it is essential to assess whether they alter responses unidirectionally. Given the skewed output distribution of MLLMs across multiple datasets, a method that merely rebalances responses may create the illusion of improved performance. However, such adjustments do not genuinely mitigate hallucinations.

**Balancing Correction and Preservation.** An effective hallucination mitigation method must strike a balance: it should correct incorrect answers while preserving correct ones. However, as shown in Figure 2, some flawed approaches, despite fixing many errors, also introduce unnecessary modifications to originally correct responses. This behavior resembles mere answer editing rather than genuine hallucination mitigation. To enhance evaluation rigor, future studies should explicitly report instances where correct responses are mistakenly altered, providing a clearer measure of a method's true effectiveness.

## 7. Conclusion

This study demonstrates that the performance improvements of contrastive decoding on the POPE benchmark largely stem from two misleading factors: (1) a unidirectional shift in the model's output distribution, which biases it toward generating "Yes" responses, artificially balancing the distribution in certain datasets, and (2) the adaptive plausibility constraint, which reduces sampling decoding to greedy search. By comparing experimental results from spurious improvement methods and contrastive decoding, we confirm that while contrastive decoding enhances performance, it ultimately fails to mitigate hallucinations.

## Impact Statement

The broader impact of this work includes fostering more transparent and accountable AI systems, particularly in applications where misinformation can have serious ethical and societal consequences, such as healthcare, legal reasoning, and scientific discovery. Our analysis underscores the importance of critical evaluation in AI research to prevent the deployment of methods that may not work as intended. While our work does not introduce new risks, it serves as a cautionary study that helps guide future research toward more robust and responsible AI development.

## References

- Bai, J., Bai, S., and et al. Qwen technical report. *arXiv preprint arXiv:2309.16609*, 2023a.
- Bai, J., Bai, S., and et al. Qwen-vl: A frontier large vision-language model with versatile abilities. *arXiv preprint arXiv:2308.12966*, 2023b.
- Bavishi, R., Elsen, E., and et al. Introducing our multimodal models, 2023. URL <https://www.adept.ai/blog/fuyu-8b>.
- Chen, K., Zhang, Z., and et al. Shikra: Unleashing multimodal llm’s referential dialogue magic. *arXiv preprint arXiv:2306.15195*, 2023a.
- Chen, L., Sinavski, O., Hünermann, J., Karnsund, A., Willmott, A. J., Birch, D., Maund, D., and Shotton, J. Driving with llms: Fusing object-level vector modality for explainable autonomous driving. *arXiv preprint arXiv:2310.01957*, 2023b.
- Chen, Z., Wang, W., and et al. How far are we to gpt-4v? closing the gap to commercial multimodal models with open-source suites. *arXiv preprint arXiv:2404.16821*, 2024a.
- Chen, Z., Wang, W., Tian, H., Ye, S., Gao, Z., Cui, E., Tong, W., Hu, K., Luo, J., Ma, Z., et al. How far are we to gpt-4v? closing the gap to commercial multimodal models with open-source suites. *Science China Information Sciences*, 67(12):220101, 2024b.
- Chen, Z., Wu, J., Wang, W., Su, W., Chen, G., Xing, S., Zhong, M., Zhang, Q., Zhu, X., Lu, L., et al. Internvl: Scaling up vision foundation models and aligning for generic visual-linguistic tasks. In *Proceedings of the IEEE/CVF Conference on Computer Vision and Pattern Recognition*, pp. 24185–24198, 2024c.
- Chen, Z., Zhao, Z., Luo, H., Yao, H., Li, B., and Zhou, J. Halc: Object hallucination reduction via adaptive focal-contrast decoding, 2024d. URL <https://arxiv.org/abs/2403.00425>.
- Chiang, W.-L. and Li, Z. e. a. Vicuna: An open-source chatbot impressing gpt-4 with 90%\* chatgpt quality. See <https://vicuna.lmsys.org> (accessed 14 April 2023), 2023.
- Dai, W. and et al, J. L. Instructblip: Towards general-purpose vision-language models with instruction tuning, 2023.
- Gunjal, A., Yin, J., and Bas, E. Detecting and preventing hallucinations in large vision language models. *arXiv preprint arXiv:2308.06394*, 2023.
- Gupta, V., Li, Z., Kortylewski, A., Zhang, C., Li, Y., and Yuille, A. Swapmix: Diagnosing and regularizing the over-reliance on visual context in visual question answering. In *Proceedings of the IEEE/CVF Conference on Computer Vision and Pattern Recognition*, pp. 5078–5088, 2022.
- Han, Y., Nie, L., Yin, J., Wu, J., and Yan, Y. Visual perturbation-aware collaborative learning for overcoming the language prior problem. *arXiv preprint arXiv:2207.11850*, 2022.
- Hu, M., Pan, S., Li, Y., and Yang, X. Advancing medical imaging with language models: A journey from n-grams to chatgpt. *arXiv preprint arXiv:2304.04920*, 2023.
- Hudson, D. A. and Manning, C. D. Gqa: A new dataset for real-world visual reasoning and compositional question answering, 2019. URL <https://arxiv.org/abs/1902.09506>.
- Huo, F., Xu, W., Zhang, Z., Wang, H., Chen, Z., and Zhao, P. Self-introspective decoding: Alleviating hallucinations for large vision-language models, 2024. URL <https://arxiv.org/abs/2408.02032>.
- Leng, S., Zhang, H., Chen, G., Li, X., Lu, S., Miao, C., and Bing, L. Mitigating object hallucinations in large vision-language models through visual contrastive decoding, 2023. URL <https://arxiv.org/abs/2311.16922>.
- Li, B., Zhang, K., and et al. Llava-next: Stronger llms supercharge multimodal capabilities in the wild, May 2024. URL <https://llava-vl.github.io/blog/2024-05-10-llava-next-stronger-llms/>.
- Li, J., Selvaraju, R., Gotmare, A., Joty, S., Xiong, C., and Hoi, S. C. H. Align before fuse: Vision and language representation learning with momentum distillation. *Advances in neural information processing systems*, 34: 9694–9705, 2021.
- Li, J., Li, D., Savarese, S., and Hoi, S. BLIP-2: Bootstrapping language-image pre-training with frozen image encoders and large language models. In *ICML*, 2023a.

- Li, X., Yin, X., Li, C., Zhang, P., Hu, X., Zhang, L., Wang, L., Hu, H., Dong, L., Wei, F., et al. Oscar: Object-semantic aligned pre-training for vision-language tasks. In *Computer Vision—ECCV 2020: 16th European Conference, Glasgow, UK, August 23–28, 2020, Proceedings, Part XXX 16*, pp. 121–137. Springer, 2020.
- Li, Y., Du, Y., Zhou, K., Wang, J., Zhao, W. X., and Wen, J.-R. Evaluating object hallucination in large vision-language models. *arXiv preprint arXiv:2305.10355*, 2023b.
- Li, Y., Du, Y., Zhou, K., Wang, J., Zhao, W. X., and Wen, J.-R. Evaluating object hallucination in large vision-language models, 2023c. URL <https://arxiv.org/abs/2305.10355>.
- Lin, T.-Y., Maire, M., and et al. Microsoft coco: Common objects in context. In *ECCV*, pp. 740–755, 2014.
- Liu, F., Lin, K., Li, L., Wang, J., Yacoob, Y., and Wang, L. Mitigating hallucination in large multi-modal models via robust instruction tuning. *arXiv preprint arXiv:2306.14565*, 2023a.
- Liu, H., Li, C., Wu, Q., and Lee, Y. J. Visual instruction tuning. In *NeurIPS*, volume 36, pp. 34892–34916, 2023b.
- Liu, H., Zhu, Y., Kato, K., Kondo, I., Aoyama, T., and Hasegawa, Y. Llm-based human-robot collaboration framework for manipulation tasks. *arXiv preprint arXiv:2308.14972*, 2023c.
- Liu, H., Li, C., Li, Y., and Lee, Y. J. Improved baselines with visual instruction tuning. In *CVPR*, pp. 26296–26306, June 2024.
- Lovenia, H., Dai, W., Cahyawijaya, S., Ji, Z., and Fung, P. Negative object presence evaluation (nope) to measure object hallucination in vision-language models. *arXiv preprint arXiv:2310.05338*, 2023.
- Mai, J., Chen, J., Li, B., Qian, G., Elhoseiny, M., and Ghanem, B. Llm as a robotic brain: Unifying egocentric memory and control. *arXiv preprint arXiv:2304.09349*, 2023.
- Meta, A. Introducing meta llama 3: The most capable openly available llm to date. *Meta AI*, 2024.
- Niu, Y., Tang, K., Zhang, H., Lu, Z., Hua, X.-S., and Wen, J.-R. Counterfactual vqa: A cause-effect look at language bias. In *Proceedings of the IEEE/CVF Conference on Computer Vision and Pattern Recognition*, pp. 12700–12710, 2021.
- Schwenk, D., Khandelwal, A., and et al. A-okvqa: A benchmark for visual question answering using world knowledge. In *ECCV*, pp. 146–162, 2022.
- Taori, R., Gulrajani, I., and et al. Stanford alpaca: an instruction-following llama model (2023). URL [https://github.com/tatsu-lab/stanford\\_alpaca](https://github.com/tatsu-lab/stanford_alpaca), 1(9), 2023.
- Touvron, H., Lavril, T., and et al. Llama: Open and efficient foundation language models. *arXiv preprint arXiv:2302.13971*, 2023a.
- Touvron, H., Martin, L., and et al. Llama 2: Open foundation and fine-tuned chat models. *arXiv preprint arXiv:2307.09288*, 2023b.
- Wang, J., Gao, Y., and Sang, J. Valid: Mitigating the hallucination of large vision language models by visual layer fusion contrastive decoding, 2024a. URL <https://arxiv.org/abs/2411.15839>.
- Wang, S., Zhao, Z., Ouyang, X., Wang, Q., and Shen, D. Chatcad: Interactive computer-aided diagnosis on medical image using large language models. *arXiv preprint arXiv:2302.07257*, 2023.
- Wang, X., Pan, J., Ding, L., and Biemann, C. Mitigating hallucinations in large vision-language models with instruction contrastive decoding, 2024b. URL <https://arxiv.org/abs/2403.18715>.
- Wu, Y., Zhao, Y., Zhao, S., Zhang, Y., Yuan, X., Zhao, G., and Jiang, N. Overcoming language priors in visual question answering via distinguishing superficially similar instances. *arXiv preprint arXiv:2209.08529*, 2022.
- Wu, Z., Wang, Z., Xu, X., Lu, J., and Yan, H. Embodied task planning with large language models. *arXiv preprint arXiv:2307.01848*, 2023.
- Yan, H., Liu, L., Feng, X., and Huang, Q. Overcoming language priors with self-contrastive learning for visual question answering. *Multimedia Tools and Applications*, 82(11):16343–16358, 2023.
- Ye, Q., Xu, H., and et al. mplug-owl: Modularization empowers large language models with multimodality. *arXiv preprint arXiv:2304.14178*, 2023.
- Zhibo, R., Huizhen, W., Muhua, Z., Yichao, W., Tong, X., and Jingbo, Z. Overcoming language priors with counterfactual inference for visual question answering. In *Proceedings of the 22nd Chinese National Conference on Computational Linguistics*, pp. 600–610, 2023.
- Zhu, D., Chen, J., Shen, X., Li, X., and Elhoseiny, M. Minigt-4: Enhancing vision-language understanding with advanced large language models. *arXiv preprint arXiv:2304.10592*, 2023.

### A. Skewness in the Output Distribution

As shown in Figure 5, the raw output distribution of MLLMs across different datasets exhibits skewness, with most datasets displaying a tendency for MLLMs to favor "No" in their outputs.

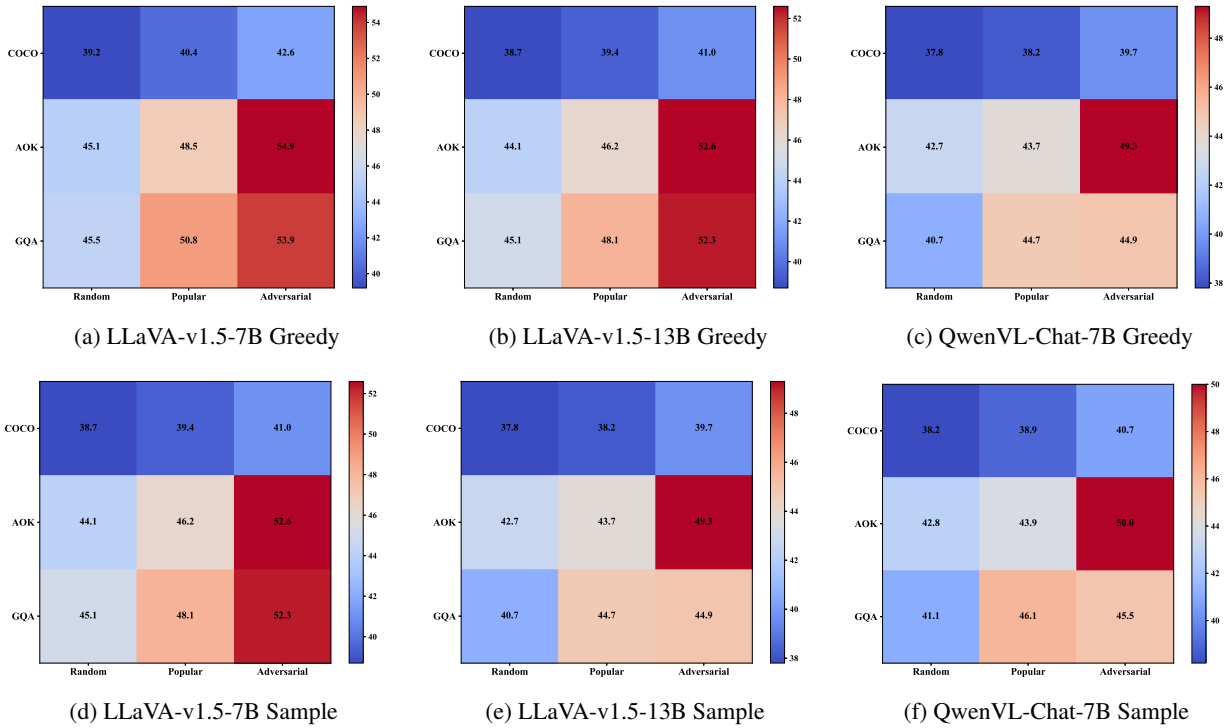


Figure 5. Skewness in the Raw Output Distribution of MLLMs across Different Datasets

## B. Additional Research on Changes in Prediction

After applying Visual Contrastive Decoding, the prediction shifts of the LLaVA-v1.5-7B model are shown in Figure 6. It is evident that across all datasets, the number of samples transitioning from Positive to Negative is significantly smaller than those shifting from Negative to Positive. This indicates that the model’s output distribution is biased towards *Yes*.

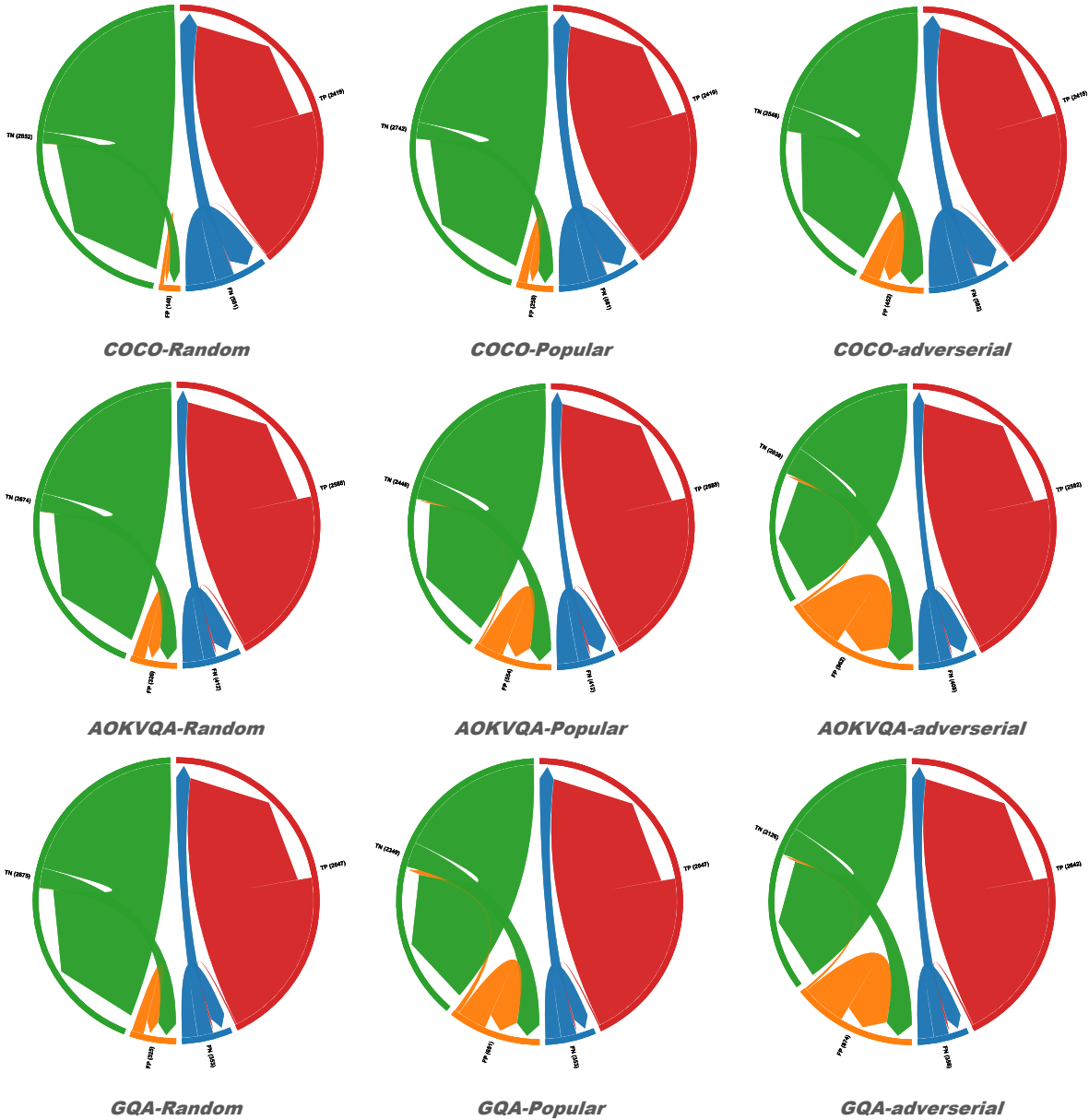


Figure 6. Changes in the distribution of model predictions across all datasets after applying Visual Contrastive Decoding.

### C. Further Experiments on Forced Distribution Adjustment

Tables 6 and 7 present the performance of Prompt-Based Adjustment (PBA) and Output Layer Modification (OLM) on the AOKVQA and GQA datasets. On both datasets, PBA and OLM maintain performance levels comparable to contrastive decoding methods. However, after surpassing the balanced distribution, accuracy declines rather than improving.

Table 6. Performance of Prompt-Based Adjustment (PBA) and Output Layer Modification (OLM) on AOKVQA dataset

Category	Decoding	LLaVA-v1.5-7B			LLaVA-v1.5-13B		
		Accuracy	F1-Score	Yes(%)	Accuracy	F1-Score	Yes(%)
Random	Greedy	88.6	88.1	45.1	88.8	88.1	44.1
	VCD	86.8	87.0	52.0	87.7	87.4	47.8
	SID	88.6	88.5	48.7	87.6	87.4	48.5
	PBA	89.0	88.5	45.9	88.7	89.0	52.8
	OLM	89.0	89.1	51.3	87.3	87.9	55.9
Popular	Greedy	85.2	85.0	48.5	86.7	86.2	46.2
	VCD	<b>82.6</b>	83.6	<b>56.2</b>	<b>85.5</b>	85.5	50.0
	SID	<b>84.1</b>	84.6	53.2	<b>85.1</b>	85.3	51.0
	PBA	<b>84.8</b>	84.8	50.1	<b>83.6</b>	84.8	57.9
	OLM	<b>82.6</b>	83.8	<b>57.7</b>	<b>83.6</b>	85.1	<b>59.5</b>
Adversarial	Greedy	78.8	79.8	54.9	80.3	80.8	52.6
	VCD	<b>75.5</b>	78.4	<b>63.6</b>	<b>79.4</b>	80.7	<b>56.4</b>
	SID	<b>77.8</b>	79.7	59.1	<b>79.2</b>	80.6	57.4
	PBA	<b>78.3</b>	79.6	56.6	<b>74.7</b>	78.3	66.8
	OLM	<b>75.0</b>	78.3	<b>65.3</b>	<b>74.8</b>	78.7	<b>68.3</b>

Table 7. Performance of Prompt-Based Adjustment (PBA) and Output Layer Modification (OLM) on GQA dataset

Category	Decoding	LLaVA-v1.5-7B			LLaVA-v1.5-13B		
		Accuracy	F1-Score	Yes(%)	Accuracy	F1-Score	Yes(%)
Random	Greedy	89.4	88.9	45.5	89.5	88.9	45.1
	VCD	88.0	88.4	53.6	88.1	88.0	49.7
	SID	88.8	88.7	49.1	88.9	88.8	49.1
	PBA	89.4	89.0	47.0	88.8	89.2	53.9
	OLM	89.4	89.7	52.9	87.1	87.9	56.9
Popular	Greedy	84.0	84.2	50.8	86.4	86.1	48.1
	VCD	<b>82.5</b>	83.9	<b>59.1</b>	<b>85.7</b>	85.5	<b>52.1</b>
	SID	<b>82.9</b>	83.8	<b>55.0</b>	<b>84.8</b>	85.2	<b>53.2</b>
	PBA	<b>83.2</b>	83.7	<b>53.1</b>	<b>84.8</b>	84.8	<b>61.9</b>
	OLM	<b>79.8</b>	82.0	<b>62.5</b>	<b>80.8</b>	83.1	<b>63.1</b>
Adversarial	Greedy	80.9	81.7	53.9	82.2	82.6	52.3
	VCD	<b>78.0</b>	80.6	63.3	<b>81.2</b>	82.4	<b>56.8</b>
	SID	<b>79.9</b>	81.3	57.8	<b>81.1</b>	82.4	<b>57.6</b>
	PBA	80.5	81.5	55.9	<b>81.1</b>	82.3	<b>67.3</b>
	OLM	<b>76.4</b>	79.6	65.9	<b>75.9</b>	79.6	<b>68.3</b>

## D. Further Experiments on Standalone Application of the Constraint

Tables 8 and 9 present the performance of the adaptive plausibility constraint on the AOKVQA and COCO datasets. When applied independently, the adaptive plausibility constraint consistently improves performance by 1.5% to 2% across both datasets.

Table 8. Impact of Adaptive Plausibility Constraint (Applied Independently) on AOKVQA Dataset

Category	Decoding	LLaVA-v1.5-7B			LLaVA-v1.5-13B		
		Accuracy	F1-Score	Yes(%)	Accuracy	F1-Score	Yes(%)
Random	sample	84.6	83.9	45.4	84.7	83.9	45.3
	VCD	85.9	86.1	51.7	86.7	86.5	48.4
	ICD	86.5	85.8	45.3	86.3	85.5	44.5
	SID	86.8	86.6	48.8	85.8	85.5	48.3
	sample <sup>†</sup>	<b>86.5</b>	<b>85.8</b>	<b>45.3</b>	<b>86.6</b>	<b>85.8</b>	<b>44.8</b>
Popular	sample	80.3	80.2	49.7	81.8	81.5	48.2
	VCD	81.3	82.4	56.2	84.1	84.2	51.0
	ICD	82.2	82.1	49.6	83.4	82.9	47.4
	SID	82.9	83.3	52.7	82.9	83.1	51.2
	sample <sup>†</sup>	<b>82.2</b>	<b>82.1</b>	<b>49.6</b>	<b>83.6</b>	<b>83.2</b>	<b>47.8</b>
Adversarial	sample	74.8	76.2	55.9	77.0	77.9	54.0
	VCD	74.8	77.6	62.8	78.4	79.7	56.4
	ICD	76.1	77.5	56.4	77.5	78.3	53.5
	SID	76.8	78.6	58.4	77.9	79.4	57.4
	sample <sup>†</sup>	<b>76.1</b>	<b>77.5</b>	<b>56.4</b>	<b>77.9</b>	<b>78.7</b>	<b>54.0</b>

Table 9. Impact of Adaptive Plausibility Constraint (Applied Independently) on COCO Dataset

Category	Decoding	LLaVA-v1.5-7B			LLaVA-v1.5-13B		
		Accuracy	F1-Score	Yes(%)	Accuracy	F1-Score	Yes(%)
Random	sample	83.6	81.8	39.8	83.9	82.3	40.8
	VCD	87.8	87.3	46.4	87.8	87.1	44.6
	ICD	85.4	83.7	39.8	85.5	83.9	40.3
	SID	86.6	85.4	41.9	86.4	85.3	42.7
	sample <sup>†</sup>	<b>85.4</b>	<b>83.7</b>	<b>39.8</b>	<b>85.5</b>	<b>84.0</b>	<b>40.6</b>
Popular	sample	82.4	80.7	41.0	83.0	81.5	41.7
	VCD	85.8	85.5	48.4	86.2	85.7	46.1
	ICD	84.1	82.5	41.1	84.6	83.1	41.2
	SID	83.6	82.7	44.9	84.4	83.5	44.8
	sample <sup>†</sup>	<b>84.1</b>	<b>82.5</b>	<b>41.1</b>	<b>84.6</b>	<b>83.1</b>	<b>41.6</b>
Adversarial	sample	80.2	78.7	43.2	81.2	79.9	43.5
	VCD	81.1	81.7	52.9	83.0	82.9	49.3
	ICD	81.8	80.5	43.3	82.6	81.3	43.2
	SID	80.9	80.4	47.5	81.8	81.3	47.3
	sample <sup>†</sup>	<b>81.8</b>	<b>80.5</b>	<b>43.3</b>	<b>82.7</b>	<b>81.5</b>	<b>43.4</b>